[**Article ID**] 1003 - 6326(2002) 06 - 1146 - 03

Deformation mechanism maps of magnesium lithium alloy and their experimental application

CAO Furrong(曹富荣), CUI Jian zhong(崔建忠), WEN Jing-lin(温景林) (Department of Material Forming and Control, School of Materials and Metallurgy, Northeastern University, Shenyang 110004, China)

[Abstract] Deformation mechanism maps for binary Mg (8~9) Li(mass fraction, %) alloy at 423~623 K were constructed in order to elucidate the internal meaning of mechanical experimental data at elevated temperatures. The models and data source used for constructing maps and constructed results are presented. It is determined through comparison of mechanical experimental data with constructed deformation mechanism maps that the dominant deformation mechanism for such alloy at 423~ 623 K is lattice diffusion controlled grain boundary sliding. The difference of such deformation mechanism maps from former ones is that dislocation quantity inside the grains participates in the model calculation, which reveals the dislocation features of different deformation mechanisms.

[Key words] magnesium alloy; dislocation; superplasticity; creep

[CLC number] TG 113

[Document code] A

1 INTRODUCTION

Deformation mechanism maps are kinds of maps disclosing the essence of rate controlling process. Many mechanism maps in different forms appear abroad since Ashby put up his first deformation mechanism maps [1~4], no deformation mechanism maps appear in China up to now.

This paper constructs deformation mechanism maps for two phase $(\alpha + \beta)$ Mg- $(8 \sim 9)$ Li alloy and obtains experimental data on superplastic deformation at elevated temperatures. The essence of deformation is expounded through the comparison of experimental data with mechanism maps. Dislocation quantity is also given at the nodal points of each mechanism zones, which helps to deepen the understanding of deformation process.

CONSTRUCTION OF DEFORMATION MECH-2 ANISM MAPS

We propose to construct deformation mechanism maps at different temperatures with Burgers' vector compensated grain size as their longitudinal coordinate and modulus compensated flow stress as their transverse coordinate. Eqns. 1~ 8 list the eight constitutive equations used to construct the maps^[3, 5]. Each of the mechanisms can be described by a constitutive equation of the following form.

$$\stackrel{\circ}{\coloneqq} A \left[\begin{array}{c} \underline{b} \\ d \end{array} \right]^p \underbrace{D}_{b^2} \left[\begin{array}{c} \underline{\sigma} \\ G \end{array} \right]^n$$

where $\dot{\epsilon}$ is the steady state creep rate; A, n, and p are materials constants, which have discrete values depending on the deformation mechanism; σ is the creep

stress; G is the shear modulus; d is the grain size; b is Burgers' vector; and D is the diffusion coefficient and is equal to either the lattice diffusion coefficient (D_1) , the dislocation pipe diffusion coefficient (D_p) , or the grain boundary diffusion coefficient ($D_{\rm gb}$). Constitutive equations used for establishing deformation mechanism $mans^{[3, 5]}$ are:

For Nabarro-Herring diffusional flow (designated as

diffusional flow
$$D_1$$
, σ^1)
$$\stackrel{\cdot}{\mathbf{E}} = K_1 \left[\frac{D_1}{d^2} \right] \left[\frac{Gb^3}{KT} \right] \left[\frac{\sigma}{G} \right] \tag{1}$$

For coble diffusional flow(designated as diffusional flow $D_{\rm gb}$, $\sigma^{\rm l}$)

$$\stackrel{\triangleright}{\epsilon} = K_2 \left[\frac{D_{\text{gh}} b}{d^3} \right] \left[\frac{G b^3}{K T} \right] \left[\frac{\sigma}{G} \right]$$
(2)

For lattice diffusion controlled grain boundary sliding (designated as superplastic GBS D_1 , σ^2)

For grain boundary diffusion controlled grain boundary sliding (designated as superplastic GBS $D_{\rm gb}$, σ^2)

For pipe diffusion controlled grain boundary sliding

(designated as dislocation slip
$$D_{\rm p}$$
, σ^4)
$$\stackrel{\epsilon}{\coloneqq} K_5 \, \operatorname{q} \left[\frac{D_{\rm p}}{d^2} \right] \left[\frac{\sigma}{G} \right]^4 \tag{5}$$

For Harper-Dorn controlled slip (designated as H-D slip D_1 , σ^1)

$$\dot{\epsilon} = K_6 \left[\frac{D_1}{b^2} \right] \left[\frac{Gb^2}{KT} \right] \left[\frac{\sigma}{G} \right]$$
(6)

For lattice diffusion controlled slip (designated as

dislocation slip
$$D_1$$
, σ^5)
$$\stackrel{\cdot}{\epsilon} = K_7 \left[\frac{D_1}{b^2} \right] \left[\frac{\sigma}{G} \right]^5 \tag{7}$$

For pipe diffusion controlled slip(designated as dislocation slip D_1 , σ^7)

where $K_1 = 14 \times 10^9$, $K_2 = 50 \times 10^9$, $K_3 = 6.4 \times 10^9$, $K_4 = 5.6 \times 10^8$, $K_5 = 3.2 \times 10^{11}$, $K_6 = 1.7 \times 10^{11}$, $K_7 = \times 10^{11}$, $K_8 = \times 10^{12}$, Meanwhile, we let dislocation quantity inside the grains n take part in the model calculation as

$$n = \frac{(1-v)\pi d\tau}{1.776Gb}$$

where v is Poisson ratio; τ is shear stress, equal to half of $o^{[6]}$.

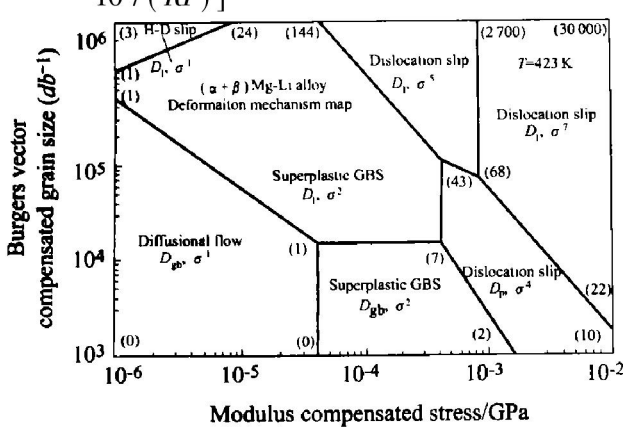
Constants used in generating maps:

G= 18. 4- 1. 082 4 × 10⁻² (T - 273) (GPa) is obtained through the regression of discrete E (modulus) data in Ref. [7] into E= 46- 2. 706 × 10⁻² (T - 273) and using G= E/2(1+v) formula.

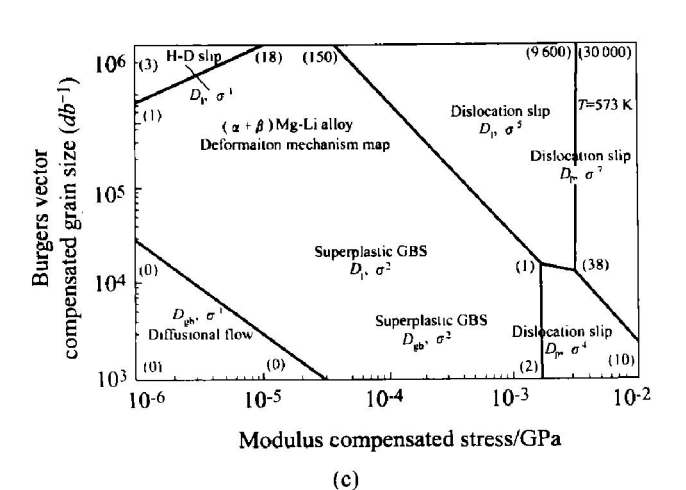
$$b = 3 \times 10^{-10} \text{ m}$$

$$a = 4, K = 1.38 \times 10^{-23} \text{ J} \cdot \text{K}^{-1}$$

$$D_{1} = 0.25 \times 10^{-4} \exp[-103.077 \times 10^{3} / (RT)]^{[8]}$$



(a)



$$D_{\rm gb} = D_{\rm p} = \begin{cases} 1 \times 10^{-4} \exp(-49.953 \times 10^{3} / (RT)) \\ \text{when } 190.74 \text{ K} < T < 364.14 \text{ K}^{[9]} \\ 1 \times 10^{-4} \exp(-67.394 \times 10^{3} / (RT)) \\ \text{when } 364.14 \text{ K} < T < 867 \text{ K} \end{cases}$$

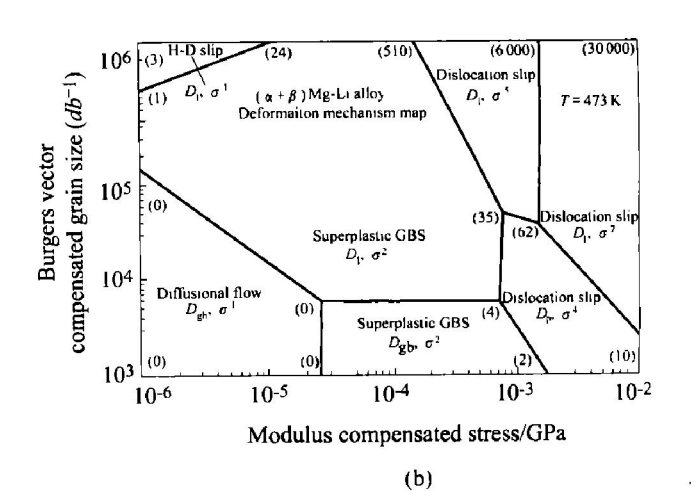
3 EXPERIMENTAL DATA

Our experimental mechanical data and data from authors abroad are processed, collected, and shown in Table $1^{[6,\ 10\sim\ 13]}$.

4 ANALYSIS OF DEFORMATION MECHANISM MAPS WITH EXPERIMENTAL DATA

Fig. 1 is the deformation mechanism maps for two phase magnesium lithium alloy constructed at $423 \sim 623$ K. Various mechanism zones are divided by name, diffusion coefficient, and stress exponent, i. e. dislocation slip $D_{\rm p}$, σ^7 indicates that the dominant deformation mechanism in such zone is dislocation slip; dislocation pipe diffusion is its diffusional process; stress exponent is 7 power. Data in parentheses at the nodal points of mechanism zone is dislocation quantity.

It can be seen through the comparison of data



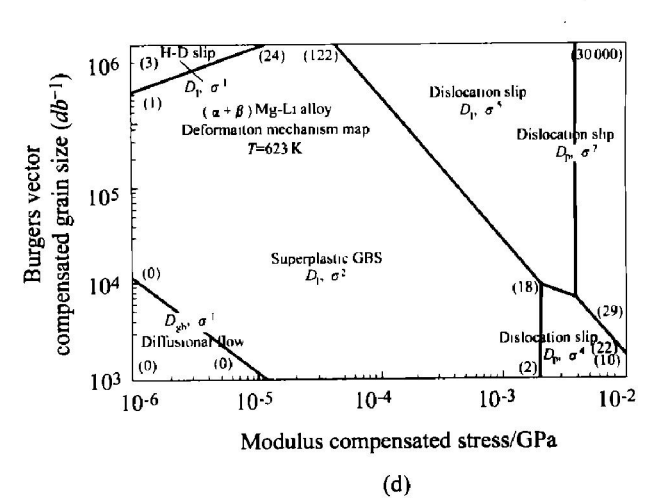


Fig. 1 Deformation mechanism maps for two phase magnesium lithium alloy constructed at different temperatures

a) -423 K; b) -473 K; c) -573 K; d) -623 K

Table 1	Experimental data for superplasticity
	of magnesium lithium alloys

Alloy	T/K	db^{-} 1 / 10^{4}	$^{\circ}G^{-1}/10^{-4}$	έ/ 10 ^{- 4} s ^{- 1}	n
Mg8Li ^[10]	623	4. 3~ 7. 8	2.0~ 3.3	8.3	5~ 15
Mg8Li1Zr	623	6. 5	2. 22	8.3	8
Mg8. 5Li ^[11]	623	3.3	2.5~ 7.8	8. 33	5~ 15
$Mg8Li^{[12]}$	573	3. 3~ 6. 6	1.6~ 4.4	0.83~ 17	3~ 16
$Mg9Li^{[13]}$	423	2. 34	2. 1~ 22. 4	0.7~ 1 800	3~ 29
$\rm Mg9Li^{[13]}$	473	1.94	6.5~ 44	0.7~ 1 800	7~ 48
Mg8. 4Li ^[6]	423	1.2	-	167	-
	473	3. 29	5.7~ 21	1.7~ 167	11~ 39
	573	4. 93	1.6~ 8.0	1.7~ 167	5~ 22
	623	6. 58	1.1~ 6.9	1.7~ 167	4~ 25

in Table 1 with Fig. 1 that our mechanical experimental data and data from different authors abroad fall into superplastic GBS D_1 , σ^2 mechanism zone, indicating that the dominant deformation mechanism for two-phase magnesium lithium alloy at 423~ 623 K is lattice diffusion controlled grain boundary sliding.

It can be seen from Fig. 1 that at lower deformation temperature, i. e. 423 K, grain boundary diffusion controlled grain boundary sliding has definite zone. As the deformation temperature rises, the lattice diffusion controlled grain boundary sliding zone increases gradually and the grain boundary diffusion controlled grain boundary sliding zone decreases gradually until the latter disappears.

It can be seen from Fig. 1 that the dislocation quantity at the nodal points of lattice diffusion controlled grain boundary sliding zone and grain boundary diffusion controlled grain boundary sliding zone is a few; the dislocation quantity at the nodal points of diffusional flow zone and above two mechanism zones is zero; the dislocation quantity at the nodal points of dislocation slip zones is large. Therefore, the dislocation feature of different mechanism zones is very obvious.

5 CONCLUSIONS

1) The deformation mechanism maps for two phase magnesium lithium alloy at 423~ 623 K are constructed. Comparison of experimental data with mechanism maps

indicates that the dominant deformation mechanism for two-phase magnesium lithium alloy at 423 ~ 623 K is lattice diffusion controlled grain boundary sliding.

2) The dislocation feature of different mechanism zones is very obvious.

[REFERENCES]

- [1] Ashby M F. A first report on deformation mechanism maps [J]. Acta Metall, 1972, 20: 887.
- [2] Frost H J, Ashby M F. Deformation Mechanism Maps[M]. Oxford: Pergamon Press, 1984. 40 - 100.
- [3] Ruano O A, Wadsworth J, Sherby O D. Deformation mechanism in an austenitic stainless steel (25Cr-20Ni) at elevated temperature [J]. J Mater Sci, 1985, 20(10): 3735.
- [4] Mishra R S, Mukerjee A K. The rate controlling deformation mechanism in high strain rate superplasticity[J]. Mater Sci Eng., 1997, 234 - 236A(3): 1023 - 1025.
- [5] Kim W J, Taleff E, Sherby O D. A proposed deformation mechanism for high strain rate superplasticity [J]. Scr Met Mater, 1995, 32(10): 1625 - 1630.
- [6] Cao F R. Preparation and Their Deformation Mechanism of Ultralight Magnesium Alloys At Elevated Temperatures [D]. Shenyang: Northeastern University, 1999: 26 - 36.
- [7] Taleff E M, Sherby O D. Mechanical behavior of fine grained Mg 6. 5Li at elevated temperature [J]. J Mater Res, 1994, 9(6): 1393.
- [8] Wolfenstine J, Gonzelez Doncel G, Sherby O D. Elevated temperature properties of Mg 14Li B particulate composites [J]. J Mater Res, 1990, 5(7): 1359 – 1361.
- [9] Taleff E M, Sherby O D. Superplastic behavior of a fine-grained Mg 9Li material at low homologous temperature [J]. J Mater Res, 1992, 7(8): 2131-2135.
- [10] Fujitani W, Higashi K, Furushiro N, et al. Effect of Zr addition on superplastic deformation of the Mg 8% Li eutectic alloy [J]. J Jpn Light Met, 1995, 45(6): 333.
- [11] Higashi K, Wolfenstine J. Microstructural evolution during superplastic flow of a binary Mg-8. 5% Li alloy [J]. Mater Lett, 1991, 10(7/8): 329.
- [12] Fujitani W, Furushiro N, Hori S. Microstructural change during superplastic deformation of the Mg 8% Li alloy[J]. J Jpn Light Met, 1992, 42(3): 125.
- [13] Metenier P, Gonzalez D G, Ruano O A, et al. Superplastic behavior of a fine-grained two phase Mg 9% Li alloy [J]. Mater Sci Eng, 1990, 125A(1/2): 195 202.

(Edited by LONG Huai-zhong)